NJC

ROYAL SOCIETY OF CHEMISTRY

PAPER

View Article Online
View Journal | View Issue

Check for updates

Cite this: *New J. Chem.*, 2021, 45, 11327

1,3,4-Oxadiazole-functionalized α-amino-phosphonates as ligands for the ruthenium-catalyzed reduction of ketones†‡

Shaima Hkiri,[ab] Christophe Gourlaouen,[c] Soufiane Touil,[b] Ali Samarat[b] and David Sémeril*[a]

Received 16th April 2021,
Accepted 19th May 2021

DOI: 10.1039/d1nj01861b

rsc.li/njc

Three α-aminophosphonates, namely diethyl[(5-phenyl-1,3,4-oxadiazol-2-ylamino)(4-trifluoromethylphenyl)methyl]phosphonate (**3a**), diethyl[(5-phenyl-1,3,4-oxadiazol-2-ylamino)(2-methoxyphenyl)methyl]phosphonate (**3b**) and diethyl[(5-phenyl-1,3,4-oxadiazol-2-ylamino)(4-nitrophenyl)methyl]phosphonate (**3c**), were synthetized *via* the Pudovik-type reaction between diethyl phosphite and imines, obtained from 5-phenyl-1,2,4-oxadiazol-2-amine and aromatic aldehydes, under microwave irradiation. Compounds **3a–c** underwent complexation with a ruthenium(II) precursor, selectively at the more basic nitrogen atom of the oxadiazole ring, leading to the corresponding ruthenium complexes **4a–c** of the formula [$RuCl_2$(**L**)(*p*-cymene)] (**L** = α-aminophosphonates **3a–c**). Complexes **4a–c** proved to be efficient catalysts for the transfer hydrogenation of ketones to alcohols. All new compounds were fully characterised by elemental analysis, infrared, mass and NMR spectroscopy. An X-ray structure of the α-aminophosphonate **3b** was obtained and revealed the presence, in the solid state, of an infinite chain of **3b** units supramolecularly interlinked. Two X-ray diffraction studies carried out on ruthenium complexes confirm the specific coordination of the electron-enricher nitrogen atom of the oxadiazole ring.

Published on 25 May 2021. Downloaded by Goteborgs Universitet on 9/1/2021 8:25:04 AM.

Introduction

α-Aminophosphonates, which are structural analogues of natural α-amino acids, have elicited considerable interest from chemists due to their wide-range of useful properties. In addition to their well-known biological activities,[1] these phosphorus compounds have gradually developed from a synthetic challenge to a directed and rational design of novel molecular ligands with outstanding metal-complexing properties. For instance, many α-aminophosphonate ligands bearing nitrogenated heterocyclic donor atoms, *i.e.* α-aminophosphonate derivatives of pyridine,[2] piperazine,[2a] quinoline[3] and imidazole[4] have demonstrated good abilities for their coordination to transition metals.

Oxadiazole derivatives, especially the 1,3,4-oxadiazole isomer, have wide pharmacological applications[5] and coordination properties.[6] Although the 1,3,4-oxadiazole moiety is present in many ruthenium complexes,[7] there are only a few examples in which the 1,3,4-oxadiazole ring is directly coordinated to the ruthenium atom.[8]

In the present investigation, we describe the synthesis and characterization of three α-aminophosphonates (**L**) incorporating a 1,3,4-oxadiazole ring, which could coordinate, *via* their electron-enriched nitrogen atom, to a ruthenium(II) precursor. The resulting ruthenium complexes of the general formula [$RuCl_2$(**L**)(η^6-*p*-cymene)][9] (Fig. 1) could be applied as catalysts for the reduction of ketones into alcohols using the transfer hydrogenation strategy, which is selective, efficient, safe and compatible with green chemistry principles.[10]

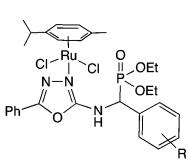

Fig. 1 Targeted [$RuCl_2$(**L**)(η^6-*p*-cymene)] complexes.

[a] *University of Strasbourg, Synthèse Organométallique et Catalyse, UMR-CNRS 7177, 4 rue Blaise Pascal, 67008 Strasbourg, France. E-mail: dsemeril@unistra.fr*
[b] *University of Carthage, Faculty of Sciences of Bizerte, LR18ES11, Laboratory of Hetero-Organic Compounds and Nanostructured Materials, 7021, Bizerte, Tunisia*
[c] *University of Strasbourg, Laboratoire de Chimie Quantique, UMR-CNRS 7177, 4 rue Blaise Pascal, 67008 Strasbourg, France*

† Dedicated to Prof. Christian Bruneau for his outstanding contribution to catalysis.

‡ Electronic supplementary information (ESI) available: Computational details and characteristic data for the compounds. CCDC 2076185–2076187. For ESI and crystallographic data in CIF or other electronic format see DOI: 10.1039/d1nj01861b

Published on 25 May 2021. Downloaded by Goteborgs Universitet on 9/1/2021 8:25:04 AM.

Results and discussion

Preparation of α-aminophosphonates

The synthesis of ruthenium complexes **4a–c** required, firstly, the preparation of the α-aminophosphonate ligands **3a–c**, respectively (Scheme 1). Precursor **1**, which was conveniently prepared according to a method earlier reported,[11] was condensed with three aromatic aldehydes, namely 4-trifluoromethylbenzaldehyde, 2-methoxybenzaldehyde and 4-nitrobenzaldehyde in order to obtain the corresponding imines **2a–c** in 87–93% yields. The Pudovik-type reaction[12] of these imine intermediates with diethyl phosphite under microwave irradiation[13] in neat conditions (115 °C and 300 W) for 10 min led to the formation of the desired α-aminophosphonates **3a–c** in 76–93% yields. The advantages of the procedure are short reaction time, high yields, and simple work up. The structures of 1,3,4-oxadiazole derivatives **3a–c** were firmly established by well-defined infrared, multinucleus NMR spectroscopy (^{1}H, ^{13}C, ^{31}P and ^{19}F), mass spectrometry and elemental analysis (see the Experimental section). Their ^{31}P{^{1}H} NMR spectra in DMSO-d_6 show a quadruplet at 19.4 ppm for **3a**, due to phosphorus/fluorine coupling ($^{7}J_{PF}$ = 2.2 Hz), and singlets at 20.7 and 18.8 ppm, for **3b** and **3c**, respectively. The ^{1}H NMR spectra revealed for the NH signals (δ = 8.87–9.18 ppm) a doublet of doublets due to a proton/proton ($^{3}J_{HH}$ = 6.0–10.2 Hz) and a phosphorus/proton ($^{3}J_{PH}$ = 1.5–3.9 Hz) vicinal coupling. The mass spectra analyses display peaks at 456.13, 418.15 and 433.13, for **3a**, **3b** and **3c**, respectively, corresponding to their $[M + H]^+$ cations with the expected isotopic profiles.

The α-aminophosphonate **3b** crystallises in the triclinic asymmetric space group $P\bar{1}$ with two distinct enantiomeric molecules (A and B molecules in which C9 and C29 have an *R* and an *S* configuration, respectively; Fig. 2). The oxadiazole and phenyl aromatic rings are almost planar with dihedral angles of 1.27° in B and 4.47° in A. The study revealed the presence in the solid state of an infinite chain of **3b** units supramolecularly interlinked. An (*R*)- and an (*S*)-molecule of **3b** dimerise *via* hydrogen bonds between their N–H and P=O moieties (H···O 2.007 Å)[14] to form a racemic dimer, which in turn self-organises *via* π–π interactions between the oxadiazole and the phenyl rings (*O*-phenyl centroid 3.369 Å and between the centroid of oxadiazole and the centroid of phenyl 3.621 Å)[15] (Fig. 3).

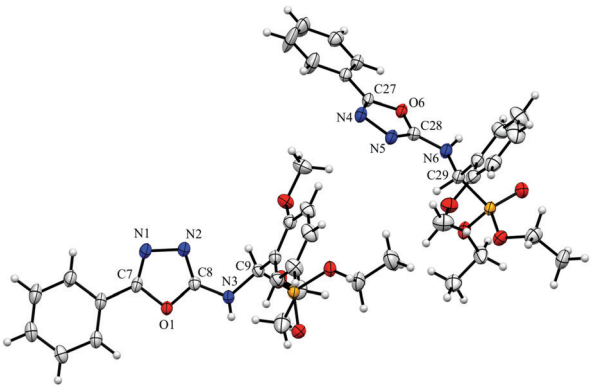

Fig. 2 ORTEP drawing of **3b**, 50% probability thermal ellipsoids, showing the two enantiomers. Important bond lengths (Å) and angles (°): N1–N2 1.419(5), N2–C8 1.304(5), C8–O1 1.365(5), O1–C7 1.385(5), C7–N1 1.275(6), C8–N3 1.341(5), N4–N5 1.419(5), N5–C28 1.297(5), C28–O6 1.365(5), O6–C27 1.384(5), C27–N4 1.281(6), C28–N6 1.347(5), C7–N1–N2 107.1(3), N1–N2–C8 104.9(3), N2–C8–O1 113.6(3), C8–O1–C7 101.5(3), O1–C7–N1 112.9(3), C27–N4–N5 106.9(3), N4–N5–C28 105.0(3), N5–C28–O6 113.8(4), C28–O6–C27 101.5(3), O6–C27–N4 112.7(4).

Preparation of ruthenium(II) complexes

The natural bond orbital charge analysis carried out on **3a** (see ESI‡) reveals that the presence of the amine moieties polarises the oxadiazole ring. If the nitrogen at position 4 in the oxadiazole ring (N1 in Fig. 2) is slightly affected, there is a strong polarisation of the nitrogen at position 3 in the oxadiazole ring (N2 in Fig. 2), which becomes more basic. Consequently, the latter nitrogen atom should be preferentially coordinated to a metal cation.

The α-aminophosphonates **3a–c** readily formed complexes with the ruthenium(II) precursor. Thus by using a Ru/L stoichiometry of 1 : 1, the reaction of **3a–c** (1 equivalent) with $[RuCl_2(p\text{-cymene})]_2$ (0.5 equivalent) in CH_2Cl_2 at room temperature for 4 h led to the formation of complexes **4a–c** in 81–92% yields (Scheme 1). The ^{31}P NMR spectra of the obtained complexes display a slight upfield shift (around 3.5 ppm) with regard to the free α-aminophosphonates. Infrared measurements show that the band at ~1600 cm^{-1} for free ligands (ν(C=N) stretching vibrations of the oxadiazole ring) shifts towards higher wave numbers by 5–10 cm^{-1} in the complexes,[8c] which confirms the coordination of a nitrogen atom to the metal centre. The mass spectra analyses, which show peaks corresponding to $[M - Cl]^+$, $[M + Na]^+$ and $[M + K]^+$ cations with the expected isotopic profiles, unambiguously confirm the coordination of the α-aminophosphonates to the ruthenium precursor. The formation of the complexes coordinated by the nitrogen in position 3 of the oxadiazole ring (noted N1 in the X-ray structures (Fig. 4 and 6)) was confirmed by single X-ray diffraction studies. The complexes crystallise in the monoclinic form with the $P2_1/n$ space group. Four molecules of complexes are present in the racemic unit cell, two ruthenium atoms are coordinated to an (*S*)-α-aminophosphonate and the two others to

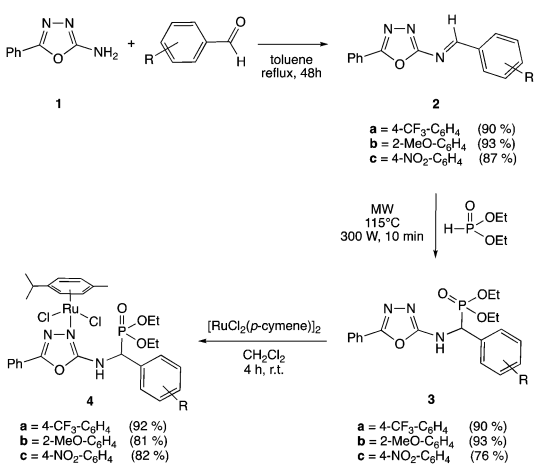

Scheme 1 Synthesis of α-aminophosphonates **3a–c** and the corresponding ruthenium complexes **4a–c**.

 This journal is © The Royal Society of Chemistry and the Centre National de la Recherche Scientifique 2021

Published on 25 May 2021. Downloaded by Goteborgs Universitet on 9/1/2021 8:25:04 AM.

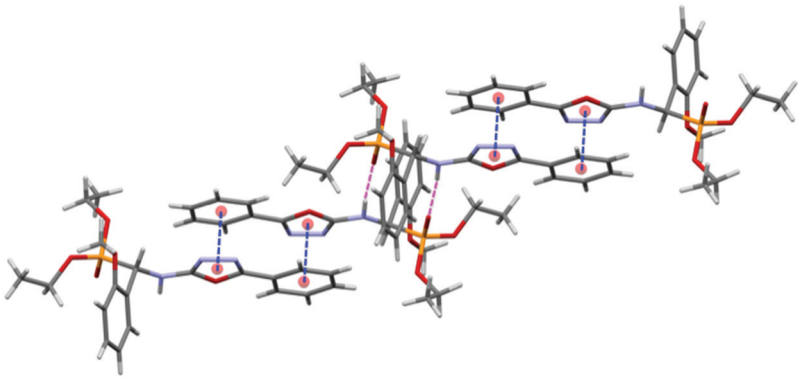

Fig. 3 Self-organised structure of **3b** *via* hydrogen bonds (magenta) and π–π (blue) interactions.

an (*R*)-α-aminophosphonate. The ruthenium atom has a typical pseudooctahedral geometry with the *p*-cymene occupying three adjacent sites of the octahedron (Ru-centroid of *p*-cymene = 1.663 and 1.656 Å in complexes **4a** and **4b**, respectively).[16] The three others sites are occupied with two chloride atoms and the α-aminophosphonate coodinated by its oxadiazole ring, which is almost orthogonal to the coordinated *p*-cymene (dihedral angle of 80.51 and 86.29° in complexes **4a** and **4b**, respectively). The bond lengths of Ru–Cl and Ru–N were found to be 2.432, 2.432 and 2.137 Å, respectively in complex **4a** and 2.429, 2.433 and 2.125 Å, respectively in complex **4b**. In the solid state, complex **4b** formation of dimers was observed, formed from a (*R*)- and a (*S*)-**3b**. The two complexes were supramolecularly linked *via* four hydrogen bonds between aromatic CH of *p*-cymene and chloride atoms (CH···Cl 2.757 and 2.806 and Å; Fig. 7). The most striking feature is the presence of a hydrogen bond involving a chlorine atom and the NH (length NH···Cl 2.280 and 2.371 Å in complexes **4a** and **4b**, respectively). The presence of a strong NH···Cl hydrogen bond was confirmed by the noncovalent interaction (NCI) analysis of the density functional theory (DFT)-optimised structure carried out on the ruthenium complex **4a** (Fig. 5). Furthermore, the calculations reveal that coordination of the oxadiazole ring by its nitrogen in position 3 (noted N1 in the X-ray structures) is favored due to higher basicity of this nitrogen atom, lower steric constraints and presence of the NH···Cl hydrogen bond (see the ESI‡).

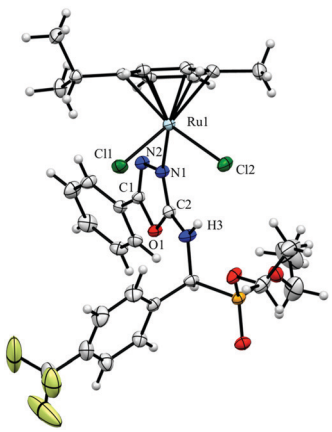

Fig. 4 ORTEP drawing of the ruthenium complex **4a** showing 50% probability thermal ellipsoids. For clarity reason, only one of the four molecules present in the unit cell is shown. Important bond lengths (Å) and angles (°): Ru1–Cl1 2.4320(5), Ru1–Cl2 2.4322(5), Ru1–N1 2.1369(15), N1–N2 1.413(2), N2–C1 1.283(2), C1–O1 1.381(2), O1–C2 1.355(2), C2–N1 1.313(2), Cl1–Ru1–N1 83.99(4), Cl1–Ru1–Cl2 87.880(18), Cl2–Ru1–N1 89.45(4) C1–N2–N1 106.25(14), N2–N1–C2 106.29(14), N1–C2–O1 111.92(15), C2–O1–C1 102.97(14), O1–C1–N2 112.58(15).

Reduction of ketones

The ruthenium complexes **4a–c** were evaluated as catalysts for reduction of ketones. The corresponding tests were performed in the presence of a base in iso-propyl alcohol (^{i}PrOH) (Scheme 2).

In order to determine the optimum catalytic conditions, the ruthenium complex **4a** (1 mol%) was used as a model catalyst in the reduction of acetophenone in ^{i}PrOH as a solvent. The reaction was studied with various bases under different conditions. Initially, the reaction was performed with K_3PO_4 as base at 80 °C for 2 h. Thus, a conversion of 67% was measured based on ^{1}H NMR analysis (Table 1, entry 1). As control experiments, no products were observed without the addition of the ruthenium complex **4a** or base. In the first series of tests, we determined the

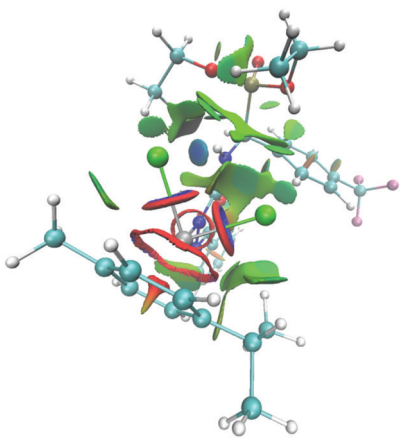

Fig. 5 Visualising the noncovalent interactions in complex **4a** with attractive electrostatic interactions in blue, attractive dispersion forces in green and steric repulsions in red.

Published on 25 May 2021. Downloaded by Goteborgs Universitet on 9/1/2021 8:25:04 AM.

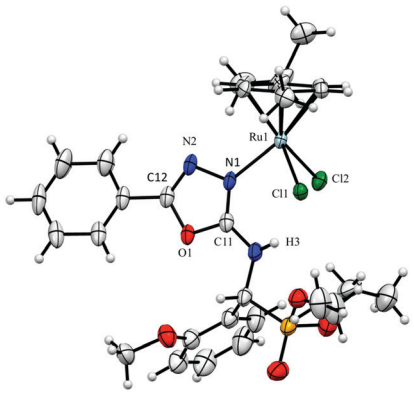

Fig. 6 ORTEP drawing of the ruthenium complex **4b** showing 50% probability level of thermal ellipsoids. For clarity reason, only one of the four molecules present in the unit cell is shown. Important bond lengths (Å) and angles (°): Ru1–Cl1 2.4330(7), Ru1–Cl2 2.4293(7), Ru1–N1 2.125(2), N1–N2 1.410(3), N2–C12 1.282(4), C12–O1 1.376(4), O1–C11 1.350(3), C11–N1 1.315(4), Cl1–Ru1–N1 84.03(7), Cl1–Ru1–Cl2 89.54(3), Cl2–Ru1–N1 87.21(7) C12–N2–N1 105.9(3), N2–N1–C11 106.5(2), N1–C11–O1 111.7(3), C11–O1–C12 103.0(2), O1–C12–N2 112.9(3).

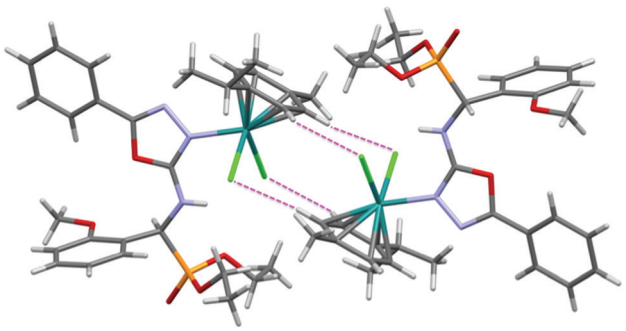

Fig. 7 Self-organised structure of **4b** *via* hydrogen bonds (magenta) interactions.

optimal base by employing NaOEt, NaOAc, KOAc, Cs_2CO_3, K_2CO_3, KOH or NaOH. As can be inferred from the results (Table 1, entries 2–8), the most efficient base was NaOH, which led to a conversion of 95% (Table 1, entry 8). Operating at lower temperature (60 °C) led to a lower conversion (17%; Table 1, entry 9). In contrast, carrying out the reaction at 100 °C increased the catalysis, and a full conversion was observed in only one hour (Table 1, entry 10). It is well established that modification of the ruthenium coordination sphere, sterically and/or electronically, has a direct effect on the catalytic outcome.[17] In fact, substitution of the CF_3 moiety by a NO_2 function on the ruthenium complex, the use of precatalyst **4c**, drastically reduced the formation of alcohol (conversion of 38%; Table 1, entry 15). Interestingly, carrying out the catalysis

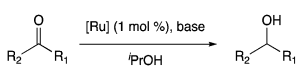

Scheme 2 Ruthenium-catalyzed reduction of ketones.

Table 1 Ruthenium-catalyzed reduction of acetophenone – screening of catalytic conditions[a]

Entry	[Ru]	Base	Time (h)	Hg	T (°C)	Conv. (%)
1	**4a**	K_3PO_4	2	No	80	67
2	**4a**	NaOEt	2	No	80	41
3	**4a**	NaOAc	2	No	80	31
4	**4a**	KOAc	2	No	80	28
5	**4a**	Cs_2CO_3	2	No	80	16
6	**4a**	K_2CO_3	2	No	80	12
7	**4a**	KOH	2	No	80	76
8	**4a**	NaOH	2	No	80	95
9	**4a**	NaOH	2	No	60	17
10	**4a**	NaOH	1	No	100	100
11	**4a**	NaOH	1	Yes	80	62
12	**4a**	NaOH	1	Yes	100	97
13	**4a**	NaOH	1	No	80	59
14	**4b**	NaOH	1	No	80	57
15	**4c**	NaOH	1	No	80	38

[a] Reagents and conditions: ruthenium complex (1 mol%), acetophenone (1.0 mmol), base (0.25 mmol), ^{i}PrOH (5 mL). The conversions were determined by ^{1}H NMR spectroscopy by integrating the CH_3 signals.

with a bulkier aromatic substituent on the ruthenium, complex **4b**, slightly reduced the effectiveness of the catalyst, conversions of 59 and 57% were measured using **4a** and **4b**, respectively (Table 1, entries 13 and 14). Note that, under our catalytic conditions, tests realised in the presence of a drop of mercury,[18] no significant change in activities were observed (Table 1, entries 11 and 12), suggesting that no ruthenium nanoparticles were present.[19]

Applying these optimised conditions (NaOH as base at 100 °C) for 2 h, the precatalyst **4a** was assigned to hydride transfer of several ketones. Seven aryl methyl ketones, namely acetophenone, 4′-chloroacetophenone, 4′-bromoacetophenone, 4′-nitroaceto-phenone, 4′-methoxyacetophenone, 2′,4′-dichloro-acetophenone and 2′-bromoacetophenone, were tested. Conversions higher than 93% were observed in the cases of acetophenone and halogenated acetophenones. For example, conversions of 97% and 93% were measured for the reduction of 4′-chloroacetophenone and 2′,4′-dichloroacetophenone or 2′-bromoacetophenone, respectively. The presence of a nitro or a methoxy substituent on the aromatic moiety led to low or moderated conversions, in fact, only 7% and 66% of 4′-nitroacetophenone and 4′-methoxyacetophenone, respectively, were reduced into the corresponding alcohol. The precatalyst **4a** efficiently carried out the hydride transfer on dialkyl and cyclic ketones, and conversions of 77%, 61% and 93% were measured starting from 3,3-dimethylbutan-2-one, cyclopentanone and cyclohexanone, respectively (Fig. 8).

Conclusions

We have shown that the synthesis of three α-aminophosphonates, in their racemic form, incorporating a 1,3,4-oxadiazole moiety, in which the nitrogen atom closer to the amine group is electrically richer than the second one. The more basic nitrogen could easily react with a ruthenium(II) precursor leading to the formation of the corresponding $[RuCl_2(\mathbf{L})(p\text{-cymene})]$ (**L** = α-aminophosphonate)

 This journal is © The Royal Society of Chemistry and the Centre National de la Recherche Scientifique 2021

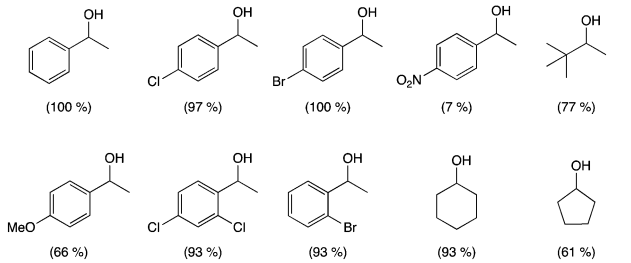

Fig. 8 Formation of alcohols, reagents and conditions: ruthenium complex **4a** (1 mol %), ketone (1.0 mmol), base (0.25 mmol), ^{i}PrOH (5 mL), 100 °C, 2 h. The conversions were determined by ^{1}H NMR spectroscopy.

Published on 25 May 2021. Downloaded by Goteborgs Universitet on 9/1/2021 8:25:04 AM.

complexes. Two X-ray diffraction studies confirm the specific coordination of the electronic richer nitrogen atom of the oxadiazole ring. The latter ruthenium(II) complexes were assigned in the transfer hydrogenation of ketones. To the best of our knowledge, the present work represents the first examples of ruthenium catalysts coordinated to a 1,3,4-oxadiazole ring. Further work is aimed at exploiting the potential chirality of α-aminophosphonates and their application as ligands in the ruthenium-catalyzed asymmetric reduction of C═O and C═N bonds.

Experimental part

All manipulations involving phosphorus derivatives were carried out under dry argon. Solvents were dried using conventional methods and were distilled immediately before use. Routine ^{1}H, ^{13}C{^{1}H}, ^{31}P{^{1}H} and ^{19}F{^{1}H} spectra were recorded on Bruker FT instruments (AC 300 and 500). ^{1}H NMR spectra were referenced to residual protonated solvents (δ = 2.50 ppm for DMSO-d_6 and δ = 7.26 ppm for $CDCl_3$). ^{13}C NMR chemical shifts are reported relative to deuterated solvents (δ = 39.52 ppm for DMSO-d_6 and δ = 77.16 ppm for $CDCl_3$). ^{31}P and ^{19}F NMR spectroscopic data are given relative to external H_3PO_4 and CCl_3F, respectively. Chemical shifts and coupling constants are reported in ppm and Hz, respectively. Infrared spectra were recorded on a Bruker FT-IR Alpha-P spectrometer. Microwave irradiation was carried out using a CEM Discover microwave synthesis system equipped with a pressure controller (17 bar). Elemental analyses were carried out using the Service de Microanalyse, Institut de Chimie, Université de Strasbourg. 5-Phenyl-1,3,4-oxadiazol-2-amine (1) was prepared by literature procedure.[11]

General procedure for the synthesis of (*E*)-1-(aryl)-*N*-(5-phenyl-1,3,4-oxadiazol-2-yl)methanimine 2a–c

In a round bottom flask equipped with a Dean Stark apparatus, a mixture of phenyl-1,3,4-oxadiazol-2-amine (**1**) (2.0 mmol) and aryl aldehyde (3.0 mmol) in toluene (20 mL) was refluxed for 48 h. After cooling to room temperature, the solvent was evaporated and the crude product was washed with cool ethanol (15 mL), filtered and dried under a vacuum to afford the desired imine.

(*E*)-1-(4-Trifluoromethylphenyl)-*N*-(5-phenyl-1,3,4-oxadiazol-2-yl)-methanimine (2a). White solid, yield 90%. ^{1}H NMR (300 MHz, DMSO-d_6): δ = 9.47 (s, 1H, N═CH), 8.33 (d, 2H, arom. CH of $C_6H_4CF_3$, $^{3}J_{HH}$ = 8.4 Hz), 8.09 (dd, 2H, arom. CH of C_6H_5, $^{3}J_{HH}$ = 7.2 Hz, $^{4}J_{HH}$ = 1.8 Hz), 7.99 (d, 2H, arom. CH of $C_6H_4CF_3$, $^{3}J_{HH}$ = 8.4 Hz), 7.68–7.60 (m, 3H, arom. CH of C_6H_5) ppm; ^{13}C{^{1}H} NMR (126 MHz, DMSO-d_6): δ = 169.48 (s, N═CH), 166.26 (s, arom. Cquat C(N)═N), 163.57 (s, arom. Cquat C(Ph)═N), 138.29 (s, arom. Cquat of $C_6H_4CF_3$), 133.46 (q, arom. Cquat *C*CF_3, $^{2}J_{CF}$ = 31.9 Hz), 132.68 (s, arom. CH), 131.31 (s, arom. CH), 129.96 (s, arom. CH), 126.98 (s, arom. CH), 126.64 (d, arom. CH, $^{3}J_{CF}$ = 3.4 Hz), 124.25 (q, CF_3, $^{1}J_{CF}$ = 273.2 Hz), 123.88 (s, arom. Cquat of C_6H_5) ppm; ^{19}F{^{1}H} NMR (282 MHz, DMSO-d_6): δ = −61.61 (s, CF_3) ppm. Elemental analysis calcd (%) for $C_{16}H_{10}ON_3F_3$ (317.27): C 60.57, H 3.18, N 13.24; found C 60.62, H 3.22, N 13.18.

(*E*)-1-(2-Methoxyphenyl)-*N*-(5-phenyl-1,3,4-oxadiazol-2-yl)-methanimine (2b). White solid, yield 93%. ^{1}H NMR (300 MHz, DMSO-d_6): δ = 9.53 (s, 1H, N═CH), 8.12 (dd, 1H, arom. CH, $^{3}J_{HH}$ = 7.8 Hz, $^{4}J_{HH}$ = 1.5 Hz), 8.06–8.02 (m, 2H, arom. CH), 7.69 (td, 1H, arom. CH, $^{3}J_{HH}$ = 7.6 Hz, $^{4}J_{HH}$ = 1.5 Hz), 7.65–7.59 (m, 3H, arom. CH), 7.25 (d, 1H, arom. CH, $^{3}J_{HH}$ = 8.4 Hz), 7.14 (t, 1H, arom. CH, $^{3}J_{HH}$ = 7.5 Hz), 3.96 (s, 3H, OCH_3) ppm; ^{13}C{^{1}H} NMR (126 MHz, DMSO-d_6): δ = 166.67 (s, arom. Cquat ortho of OCH_3), 164.34 (s, N═CH), 162.75 (s, arom. Cquat C(Ph)═N), 160.96 (s, arom. Cquat C(N)═N), 136.53 (s, arom. CH), 131.95 (s, arom. CH), 129.44 (s, arom. CH), 127.63 (s, arom. CH), 126.36 (s, arom. CH), 123.59 (s, arom. Cquat), 122.10 (s, arom. Cquat), 121.11 (s, arom. CH), 112.58 (s, arom. CH), 56.13 (s, OCH_3) ppm. Elemental analysis calcd (%) for $C_{16}H_{13}O_2N_3$ (279.29): C 68.81, H 4.69, N 15.04; found C 68.84, H 4.73, N 14.99.

(*E*)-1-(4-Nitrophenyl)-*N*-(5-phenyl-1,3,4-oxadiazol-2-yl)-methanimine (2c). Yellow solid, yield 87%. ^{1}H NMR (300 MHz, DMSO-d_6): δ = 9.51 (s, 1H, N═CH), 8.44 (d, 2H, arom. CH of $C_6H_4NO_2$, $^{3}J_{HH}$ = 9.0 Hz), 8.37 (d, 2H, arom. CH of $C_6H_4NO_2$, $^{3}J_{HH}$ = 9.0 Hz), 8.09 (d, 2H, arom. CH of C_6H_5, $^{3}J_{HH}$ = 8.1 Hz), 7.68–7.62 (m, 3H, arom. CH of C_6H_5) ppm; ^{13}C{^{1}H} NMR (126 MHz, DMSO-d_6): δ = 168.44 (s, N═CH), 165.69 (s, arom. Cquat C(N)═N), 163.21 (s, arom. Cquat C(Ph)═N), 150.27 (q, arom. Cquat CNO_2), 139.60 (s, arom. Cquat of $C_6H_4NO_2$), 132.31 (s, arom. CH), 131.31 (s, arom. CH), 129.54 (s, arom. CH), 126.57 (s, arom. CH), 124.34 (s, arom. CH), 123.38 (s, arom. Cquat of C_6H_5) ppm. Elemental analysis calcd (%) for $C_{15}H_{10}O_3N_4$ (294.27): C 61.22, H 3.43, N 19.04; found C 61.18, H 3.35, N 18.97.

General procedure for the synthesis of diethyl[(5-phenyl-1,3,4-oxadiazol-2-ylamino)(aryl)methyl]phosphonate 3a–c

In a round bottom flask, a mixture of (*E*)-1-(aryl)-*N*-(5-phenyl-1,3,4-oxadiazol-2-yl)methanimine (**2**) (1.0 mmol) and diethyl phosphite (0.25 mL, 2.0 mmol) was added and irradiated under microwave under neat conditions at 115 °C for 10 min at 300 W. After cooling to room temperature, the crude product was washed with EtO_2 (3 × 10 mL), filtered and dried under a vacuum to afford a white solid. In the case of **3c**, the crude

Published on 25 May 2021. Downloaded by Goteborgs Universitet on 9/1/2021 8:25:04 AM.

product was purified by column chromatography (EtOAc/Et_2O, 50 : 50, v/v) to afford a white solid.

Diethyl[(5-phenyl-1,3,4-oxadiazol-2-ylamino)(4-trifluoromethylphenyl)methyl]phosphonate (3a). Yield 90%. ^{1}H NMR (300 MHz, DMSO-d_6): δ = 9.14 (dd, 1H, NH, $^3J_{HH}$ = 6.0 Hz, $^3J_{PH}$ = 1.5 Hz), 7.85–7.77 (m, 6H, arom. CH), 7.56–7.51 (m, 3H, arom. CH), 5.38 (dd, 1H, CHP, $^2J_{PH}$ = 13.5 Hz, $^3J_{HH}$ = 5.7 Hz), 4.08–3.88 (m, 4H, OCH_2CH$_3$), 1.18 (t, 3H, OCH$_2$CH_3, $^3J_{HH}$ = 4.2 Hz), 1.10 (t, 3H, OCH$_2$CH_3, $^3J_{HH}$ = 4.2 Hz) ppm; ^{13}C{^{1}H} NMR (126 MHz, DMSO-d_6): δ = 162.95 (d, arom. Cquat *para* of CF_3, $^2J_{CP}$ = 11.2 Hz), 158.41 (s, arom. Cquat C(Ph)═N), 140.37 (s, arom. Cquat C(NH)═N), 130.80 (s, arom. CH), 129.30 (s, arom. CH), 128.92 (d, arom. CH, $^3J_{CP}$ = 4.6 Hz), 128.43 (q, arom. Cquat *C*CF_3, $^2J_{CF}$ = 32.8 Hz), 125.30 (s, arom. CH), 125.14 (s, arom. CH), 124.20 (q, CF_3, $^1J_{CF}$ = 272.5 Hz), 123.94 (s, arom. Cquat of C_6H_5), 62.91 (d, O*C*H$_2$CH$_3$, $^2J_{CP}$ = 23.1 Hz), 62.86 (d, O*C*H$_2$CH$_3$, $^2J_{CP}$ = 22.9 Hz), 54.10 (d, CHP, $^1J_{CP}$ = 153.3 Hz), 16.16 (d, OCH$_2$*C*H$_3$, $^3J_{CP}$ = 19.1 Hz), 16.12 (d, OCH$_2$*C*H$_3$, $^3J_{CP}$ = 19.3 Hz) ppm; ^{31}P{^{1}H} NMR (121 MHz, DMSO-d_6): δ = 19.4 (q, P(O), $^7J_{PF}$ = 2.2 Hz) ppm; ^{19}F{^{1}H} NMR (282 MHz, DMSO-d_6): δ = −60.97 (d, CF_3, $^7J_{PF}$ = 2.0 Hz) ppm. IR: ν = 1600 cm^{-1} (C═N). MS (ESI-TOF): *m*/*z* = 456.13 [M + H]$^+$, 478.11 [M + Na]$^+$, 494.09 [M + K]$^+$ (expected isotopic profiles). Elemental analysis calcd (%) for $C_{20}H_{21}O_4N_3F_3P$ (455.37): C 52.75, H 4.65, N 9.23; found C 52.71, H 4.59, N 9.20.

Diethyl[(5-phenyl-1,3,4-oxadiazol-2-ylamino)(2-methoxyphenyl)methyl]phosphonate (3b). Yield 93%. ^{1}H NMR (300 MHz, DMSO-d_6): δ = 8.87 (dd, 1H, NH, $^3J_{HH}$ = 10.2 Hz, $^3J_{PH}$ = 2.7 Hz), 7.81–7.78 (m, 2H, arom. CH), 7.62 (dt, 1H, arom. CH, $^3J_{HH}$ = 7.8 Hz, $^4J_{HH}$ = 2.0 Hz), 7.56–7.52 (m, 3H, arom. CH), 7.34–7.28 (m, 1H, arom. CH), 7.03 (d, 1H, arom. CH, $^3J_{HH}$ = 8.1 Hz), 6.98 (t, 1H, arom. CH, $^3J_{HH}$ = 7.5 Hz), 5.69 (dd, 1H, CHP, $^2J_{PH}$ = 21.3 Hz, $^3J_{HH}$ = 10.2 Hz), 4.09–3.99 (m, 2H, OCH$_2$CH$_3$), 3.95–3.83 (m, 1H, OCH_2CH$_3$), 3.86 (s, 3H, OCH$_3$), 3.82–3.69 (m, 1H, OCH_2CH$_3$), 1.18 (t, 3H, $^3J_{HH}$ = 7.1 Hz, OCH$_2$CH_3), 1.04 (t, 3H, $^3J_{HH}$ = 7.1 Hz, OCH$_2$CH_3) ppm; ^{13}C{^{1}H} NMR (126 MHz, DMSO-d_6): δ = 163.08 (d, arom. Cquat ortho of OCH$_3$, $^2J_{CP}$ = 10.1 Hz), 158.12 (s, arom. Cquat C(Ph)═N), 156.37 (d, arom. Cquat C(NH)═N, $^3J_{CP}$ = 5.7 Hz), 130.69 (s, arom. CH), 129.32 (s, arom. CH), 128.74 (d, arom. CH, $^3J_{CP}$ = 3.5 Hz), 125.17 (s, arom. CH), 124.03 (s, arom. Cquat of C_6H_5), 123.67 (s, arom. Cquat COCH$_3$), 120.34 (s, arom. CH), 110.99 (s, arom. CH), 62.49 (d, O*C*H$_2$CH$_3$, $^2J_{CP}$ = 5.8 Hz), 55.83 (s, OCH$_3$), 47.17 (d, CHP, $^1J_{CP}$ = 158.3 Hz), 16.24 (d, OCH$_2$*C*H$_3$, $^3J_{CP}$ = 5.4 Hz), 16.01 (d, OCH$_2$*C*H$_3$, $^3J_{CP}$ = 5.4 Hz) ppm; ^{31}P{^{1}H} NMR (121 MHz, DMSO-d_6): δ = 20.7 (s, P(O)) ppm. IR: ν = 1604 cm^{-1} (C═N). MS (ESI-TOF): *m*/*z* = 418.15 [M + H]$^+$, 440.13 [M + Na]$^+$, 456.11 [M + K]$^+$ (expected isotopic profiles). Elemental analysis calcd (%) for $C_{20}H_{24}O_5N_3P$ (417.40): C 57.55, H 5.80, N 10.07; found C 57.45, H 5.72, N 10.01.

Diethyl[(5-phenyl-1,3,4-oxadiazol-2-ylamino)(4-nitrophenyl)methyl]phosphonate (3c). Yield 76%. ^{1}H NMR (300 MHz, DMSO-d_6): δ = 9.18 (dd, 1H, NH, $^3J_{HH}$ = 9.9 Hz, $^3J_{PH}$ = 3.9 Hz), 8.27 (d, 2H, arom. CH, $^3J_{HH}$ = 8.4 Hz), 7.86–7.82 (m, 4H, arom. CH), 7.55–7.53 (m, 3H, arom. CH), 5.46 (dd, 1H, CHP, $^2J_{PH}$ = 23.1 Hz, $^3J_{HH}$ = 9.9 Hz), 4.12–3.89 (m, 4H, OCH_2CH$_3$), 1.18 (t, 3H, OCH$_2$CH_3, $^3J_{HH}$ = 7.1 Hz), 1.12 (t, 3H, OCH$_2$CH_3, $^3J_{HH}$ = 7.1 Hz) ppm; ^{13}C{^{1}H} NMR (126 MHz, DMSO-d_6): δ = 162.90 (d, arom. Cquat para of NO_2, $^2J_{CP}$ = 11.1 Hz), 158.50 (s, arom. Cquat C(Ph)═N), 147.16 (d, arom. Cquat C(NH)═N, $^3J_{CP}$ = 2.4 Hz), 143.36 (s, arom. Cquat CNO_2), 130.87 (s, arom. CH), 129.39 (s, arom. CH), 129.33 (s, arom. CH), 125.35 (s, arom. CH), 123.91 (s, arom. Cquat of C_6H_5), 123.39 (s, arom. CH), 63.08 (d, O*C*H$_2$CH$_3$, $^2J_{CP}$ = 22.7 Hz), 63.03 (d, O*C*H$_2$CH$_3$, $^2J_{CP}$ = 22.6 Hz), 54.11 (d, CHP, $^1J_{CP}$ = 152.5 Hz), 16.20 (d, OCH$_2$*C*H$_3$, $^3J_{CP}$ = 15.5 Hz), 16.16 (d, OCH$_2$*C*H$_3$, $^3J_{CP}$ = 15.7 Hz) ppm; ^{31}P{^{1}H} NMR (121 MHz, DMSO-d_6): δ = 18.8 (s, P(O)) ppm. IR: ν = 1601 cm^{-1} (C═N). MS (ESI-TOF): *m*/*z* = 433.13 [M + H]$^+$, 455.11 [M + Na]$^+$, 471.08 [M + K]$^+$ (expected isotopic profiles). Elemental analysis calcd (%) for $C_{19}H_{21}O_6N_4P$ (432.37): C 52.78, H 4.90, N 12.96; found C 52.84, H 4.94, N 12.91.

General procedure for the synthesis of the ruthenium(II) complexes 4a–c

To a stirred solution (CH_2Cl_2, 15 mL) of diethyl[(5-phenyl-1,3,4-oxadiazol-2-ylamino)(aryl)methyl] phosphonate (**3a–c**) (1.00 mmol) was added a solution of [$RuCl_2$(*p*-cymene)]$_2$ (0.306 g, 0.05 mmol) in CH_2Cl_2 (15 mL). After stirring at room temperature for 4 h, the reaction mixture was concentrated to *ca.* 1 mL, upon which *n*-hexane (50 mL) was added. The orange/red precipitate was separated by filtration and dried under a vacuum.

Dichloro-{diethyl[(5-phenyl-1,3,4-oxadiazol-2-ylamino)-(4-trifluoro-methylphenyl)methyl]phosphonate}(*p*-cymene)-ruthenium(II) (4a). Yield 92%. ^{1}H NMR (500 MHz, $CDCl_3$): δ = 8.46 (dd, 1H, NH, $^3J_{HH}$ = 9.0 Hz, $^3J_{PH}$ = 8.0 Hz), 7.73–7.71 (m, 4H, arom. CH), 7.60 (d, 2H, arom. CH, $^3J_{HH}$ = 8.0 Hz), 7.52–7.45 (m, 3H, arom. CH), 5.67 and 5.40 (AA′BB′ spin system, 2H, arom. CH of *p*-cymene, $^3J_{HH}$ = 6.0 Hz), 5.65 and 5.38 (AA′BB′ spin system, 2H, arom. CH of *p*-cymene, $^3J_{HH}$ = 5.5 Hz), 5.00 (dd, 1H, CHP, $^2J_{PH}$ = 23.0 Hz, $^3J_{HH}$ = 9.0 Hz), 4.28–4.16 (m, 2H, OCH_2CH$_3$), 4.03–3.91 (m, 2H, OCH_2CH$_3$), 3.14 (hept, 1H, C*H*(CH$_3$)$_2$, $^3J_{HH}$ = 6.7 Hz), 2.33 (s, 3H, CH_3 of *p*-cymene), 1.32 (d, 3H, CH(CH_3)$_2$, $^3J_{HH}$ = 6.7 Hz), 1.31 (d, 3H, CH(CH_3)$_2$, $^3J_{HH}$ = 6.7 Hz), 1.30 (t, 3H, OCH$_2$CH_3, $^3J_{HH}$ = 6.5 Hz), 1.20 (t, 3H, OCH$_2$CH_3, $^3J_{HH}$ = 7.0 Hz) ppm; ^{13}C{^{1}H} NMR (126 MHz, $CDCl_3$): δ = 162.20 (d, arom. Cquat para of CF_3, $^2J_{CP}$ = 11.8 Hz), 156.67 (s, arom. Cquat C(Ph)═N), 138.47 (s, arom. Cquat C(NH)═N), 131.69 (s, arom. CH), 129.26 (s, arom. CH), 128.37 (d, arom. CH, $^3J_{CP}$ = 4.5 Hz), 130.42 (q, arom. Cquat *C*CF_3, $^2J_{CF}$ = 30.5 Hz), 125.91 (s, arom. CH), 125.67 (s, arom. CH), 124.08 (q, CF_3, $^1J_{CF}$ = 273.2 Hz), 122.98 (s, arom. Cquat of C_6H_5), 103.14 (s, arom. Cquat of *p*-cymene), 98.97 (s, arom. Cquat of *p*-cymene), 83.91 (s, arom. CH of *p*-cymene), 83.82 (s, arom. CH of *p*-cymene), 81.49 (s, arom. CH of *p*-cymene), 81.37 (s, arom. CH of *p*-cymene), 64.72 (d, O*C*H$_2$CH$_3$, $^2J_{CP}$ = 7.1 Hz), 64.33 (d, O*C*H$_2$CH$_3$, $^2J_{CP}$ = 7.3 Hz), 55.68 (d, CHP, $^1J_{CP}$ = 152.5 Hz), 30.78 (s, *C*H(CH$_3$)$_2$), 22.45 (s, CH(*C*H$_3$)$_2$), 22.41 (s, CH(*C*H$_3$)$_2$), 19.00 (s, CH_3 of *p*-cymene), 16.61 (d, OCH$_2$*C*H$_3$, $^3J_{CP}$ = 5.3 Hz), 16.58 (d, OCH$_2$*C*H$_3$, $^3J_{CP}$ = 4.6 Hz) ppm; ^{31}P{^{1}H} NMR (121 MHz, $CDCl_3$): δ = 15.8 (q, P(O), $^7J_{PF}$ = 2.2 Hz) ppm; ^{19}F{^{1}H} NMR (282 MHz, $CDCl_3$): δ = −62.68 (d, CF_3, $^7J_{PF}$ = 2.2 Hz) ppm. IR: ν = 1650 cm^{-1} (C═N). MS (ESI-TOF): *m*/*z* = 726.10 [M − Cl]$^+$, 784.06 [M + Na]$^+$, 800.04 [M + K]$^+$ (expected isotopic profiles). Elemental analysis calcd (%) for $C_{30}H_{35}O_4N_3F_3PCl_2Ru$ (761.56): C 47.31, H 4.63, N 5.52; found C 47.24, H 4.55, N 5.48.

 This journal is © The Royal Society of Chemistry and the Centre National de la Recherche Scientifique 2021

Published on 25 May 2021. Downloaded by Goteborgs Universitet on 9/1/2021 8:25:04 AM.

Dichloro-{diethyl[(5-phenyl-1,3,4-oxadiazol-2-ylamino)-(2-methoxyphenyl)methyl]phosphonate}(*p*-cymene)ruthenium(II) (4b). Yield 81%. ^{1}H NMR (500 MHz, $CDCl_3$): δ = 8.37 (dd, 1H, NH, $^3J_{HH}$ = 6.0 Hz, $^3J_{PH}$ = 9.0 Hz), 7.78 (d, 2H, arom. CH, $^3J_{HH}$ = 6.5 Hz), 7.55 (d, 1H, arom. CH, $^3J_{HH}$ = 7.5 Hz), 7.51–7.47 (m, 3H, arom. CH), 7.21 (t, 1H, arom. CH, $^3J_{HH}$ = 7.7 Hz), 6.94 (t, 1H, arom. CH, $^3J_{HH}$ = 7.5 Hz), 6.84 (d, 1H, arom. CH, $^3J_{HH}$ = 8.0 Hz), 5.63 and 5.36 (AA′BB′ spin system, 2H, arom. CH of *p*-cymene, $^3J_{HH}$ = 6.0 Hz), 5.61 and 5.34 (AA′BB′ spin system, 2H, arom. CH of *p*-cymene, $^3J_{HH}$ = 6.0 Hz), 5.54 (dd, 1H, CHP, $^2J_{PH}$ = 22.0 Hz, $^3J_{HH}$ = 9.0 Hz), 4.23–4.13 (m, 2H, OCH_2CH$_3$), 4.07–3.01 (m, 2H, OCH_2CH$_3$), 3.90 (s, 3H, OCH$_3$), 3.12 (hept, 1H, CH(CH$_3$)$_2$, $^3J_{HH}$ = 6.7 Hz), 2.30 (s, 3H, CH$_3$ of *p*-cymene), 1.29 (d, 3H, CH(CH_3)$_2$, $^3J_{HH}$ = 6.7 Hz), 1.28 (d, 3H, CH(CH_3)$_2$, $^3J_{HH}$ = 6.7 Hz), 1.26 (t, 3H, OCH$_2$CH_3, $^3J_{HH}$ = 6.5 Hz), 1.24 (t, 3H, OCH$_2$CH_3, $^3J_{HH}$ = 7.5 Hz) ppm; ^{13}C{^{1}H} NMR (126 MHz, $CDCl_3$): δ = 162.26 (d, arom. Cquat ortho of OCH$_3$, $^2J_{CP}$ = 10.6 Hz), 156.77 (d, arom. Cquat C(NH)═N, $^3J_{CP}$ = 5.6 Hz), 156.30 (s, arom. Cquat C(Ph)═N), 131.35 (s, arom. CH), 129.54 (d, arom. CH, $^4J_{CP}$ = 5.1 Hz), 129.51 (d, arom. CH, $^3J_{CP}$ = 7.5 Hz), 129.11 (s, arom. CH), 125.86 (s, arom. CH), 123.38 (s, arom. Cquat *C*OCH$_3$), 122.73 (s, arom. Cquat of C$_6$H$_5$), 121.17 (s, arom. CH), 110.63 (s, arom. CH), 103.00 (s, arom. Cquat of *p*-cymene), 98.67 (s, arom. Cquat of *p*-cymene), 83.74 (s, arom. CH of *p*-cymene), 83.72 (s, arom. CH of *p*-cymene), 81.45 (s, arom. CH of *p*-cymene), 81.42 (s, arom. CH of *p*-cymene), 64.05 (d, O*C*H$_2$CH$_3$, $^2J_{CP}$ = 7.1 Hz), 63.81 (d, O*C*H$_2$CH$_3$, $^2J_{CP}$ = 7.3 Hz), 55.96 (s, OCH$_3$), 49.39 (d, CHP, $^1J_{CP}$ = 158.3 Hz), 30.71 (s, *C*H(CH$_3$)$_2$), 22.42 (s, CH(*C*H$_3$)$_2$), 22.38 (s, CH(*C*H$_3$)$_2$), 18.93 (s, CH$_3$ of *p*-cymene), 16.63 (d, OCH$_2$*C*H$_3$, $^3J_{CP}$ = 4.4 Hz), 16.60 (d, OCH$_2$*C*H$_3$, $^3J_{CP}$ = 5.0 Hz) ppm; ^{31}P{^{1}H} NMR (121 MHz, $CDCl_3$): δ = 17.5 (s, P(O)) ppm. IR: ν = 1644 cm^{-1} (C═N). MS (ESI-TOF): *m*/*z* = 688.13 [M − Cl]$^+$, 746.09 [M + Na]$^+$, 762.06 [M + K]$^+$ (expected isotopic profiles). Elemental analysis calcd (%) for $C_{30}H_{38}O_5N_3PCl_2Ru$ (723.59): C 49.80, H 5.29, N 5.81; found C 49.73, H 5.19, N 5.76.

Dichloro-{diethyl[(5-phenyl-1,3,4-oxadiazol-2-ylamino)-(4-nitrophenyl)methyl]phosphonate}(*p*-cymene)ruthenium(II) (4c). Yield 82%. ^{1}H NMR (500 MHz, $CDCl_3$): δ = 8.53 (dd, 1H, NH, $^3J_{HH}$ = 8.5 Hz, $^3J_{PH}$ = 8.0 Hz), 8.19 (d, 2H, arom. CH of $O_2NC_6H_4$, $^3J_{HH}$ = 8.0 Hz), 7.81 (d, 2H, arom. CH, $^3J_{HH}$ = 7.5 Hz), 7.72 (d, 2H, arom. CH of $O_2NC_6H_4$, $^3J_{HH}$ = 8.0 Hz), 7.53–7.45 (m, 3H, arom. CH), 5.68 and 5.40 (AA′BB′ spin system, 2H, arom. CH of *p*-cymene, $^3J_{HH}$ = 5.5 Hz), 5.65 and 5.39 (AA′BB′ spin system, 2H, arom. CH of *p*-cymene, $^3J_{HH}$ = 6.0 Hz), 5.05 (dd, 1H, CHP, $^2J_{PH}$ = 23.5 Hz, $^3J_{HH}$ = 8.5 Hz), 4.28–4.19 (m, 2H, OCH_2CH$_3$), 4.04–3.95 (m, 2H, OCH_2CH$_3$), 3.14 (hept, 1H, CH(CH$_3$)$_2$, $^3J_{HH}$ = 6.7 Hz), 2.33 (s, 3H, CH$_3$ of *p*-cymene), 1.32 (d, 3H, CH(CH_3)$_2$, $^3J_{HH}$ = 6.7 Hz), 1.31 (d, 3H, CH(CH_3)$_2$, $^3J_{HH}$ = 6.7 Hz), 1.30 (t, 3H, OCH$_2$CH_3, $^3J_{HH}$ = 7.2 Hz), 1.21 (t, 3H, OCH$_2$CH_3, $^3J_{HH}$ = 7.0 Hz) ppm; ^{13}C{^{1}H} NMR (126 MHz, $CDCl_3$): δ = 162.19 (d, arom. Cquat para of NO$_2$, $^2J_{CP}$ = 11.5 Hz), 156.79 (s, arom. Cquat C(Ph)═N), 147.89 (d, arom. Cquat C(NH)═N, $^3J_{CP}$ = 2.8 Hz), 141.91 (d, arom. Cquat CNO$_2$, $^5J_{CP}$ = 2.1 Hz), 131.81 (s, arom. CH), 129.31 (s, arom. CH), 128.99 (d, arom. CH, $^3J_{CP}$ = 4.4 Hz), 125.91 (s, arom. CH), 123.88 (s, arom. CH), 122.89 (s, arom. Cquat of C$_6$H$_5$), 103.24 (s, arom. Cquat of *p*-cymene), 99.05 (s, arom. Cquat of *p*-cymene), 83.92 (s, arom. CH of *p*-cymene), 83.74 (s, arom. CH of *p*-cymene), 81.50 (s, arom. CH of *p*-cymene), 81.31 (s, arom. CH of *p*-cymene), 64.76 (d, O*C*H$_2$CH$_3$, $^2J_{CP}$ = 7.3 Hz), 64.48 (d, O*C*H$_2$CH$_3$, $^2J_{CP}$ = 7.3 Hz), 55.68 (d, CHP, $^1J_{CP}$ = 151.4 Hz), 30.81 (s, *C*H(CH$_3$)$_2$), 22.46 (s, CH(*C*H$_3$)$_2$), 22.40 (s, CH(*C*H$_3$)$_2$), 18.99 (s, CH$_3$ of *p*-cymene), 16.61 (d, OCH$_2$*C*H$_3$, $^3J_{CP}$ = 5.0 Hz), 16.58 (d, OCH$_2$*C*H$_3$, $^3J_{CP}$ = 4.4 Hz) ppm; ^{31}P{^{1}H} NMR (121 MHz, $CDCl_3$): δ = 15.1 (s, P(O)) ppm. IR: ν = 1650 cm^{-1} (C═N). MS (ESI-TOF): *m*/*z* = 703.10 [M − Cl]$^+$, 761.06 [M + Na]$^+$, 777.04 [M + K]$^+$ (expected isotopic profiles). Elemental analysis calcd (%) for $C_{29}H_{35}O_6N_4PCl_2Ru$ (738.56): C 47.16, H 4.78, N 7.59; found C 47.08, H 4.66, N 7.54.

General procedure for the ruthenium-catalyzed reduction of ketones

A 10 mL-Schlenk tube was filled with the ruthenium precursor (1.0 mol %), NaOH (0.25 mol) and ketone (1.0 mmol). ^{i}PrOH (5 mL) was then added. The reaction mixture was stirred at 100 °C for 2 h. An aliquot (0.25 mL) of the resulting solution was then passed through a Millipore filter, the solvent was then removed under a vacuum and the resulting crude solution was analyzed by ^{1}H NMR spectroscopy.

X-Ray crystal structure analysis

Single crystals of **3b** suitable for X-ray analysis were obtained by slow evaporation of a diethyl ether solution of the crude reaction mixture. Crystal data: $C_{20}H_{24}N_3O_5P$, M_r = 417.40 g mol^{-1}, triclinic, space group $P\bar{1}$, a = 8.8977(11) Å, b = 12.5369(14) Å, c = 19.5140(20) Å, α = 90.816(4)°, β = 94.235(4)°, γ = 103.384(4)°, V = 2110.8(4) Å^3, Z = 4, D = 1.313 g cm^{-3}, μ = 0.166 mm^{-1}, F(000) = 880, T = 120(2) K. The sample (0.220 × 0.200 × 0.180) was studied on a Bruker PHOTON-III CPAD using Mo-K$_\alpha$ radiation (λ = 0.71073 Å). The data collection ($2\theta_{max}$ = 28.012°, omega scan frames by using 0.7° omega rotation and 30 s per frame, range *hkl*: *h* −11,11 *k* −16,16 *l* −25,25) gave 95 599 reflections. The structure was solved with SHELXT-2014/5,[20] which revealed the non-hydrogen atoms of the molecule. After anisotropic refinement, all of the hydrogen atoms were found with a Fourier difference map. The structure was refined with SHELXL-2014/7[21] by the full-matrix least-square techniques (the use of F square magnitude; x, y, z, β_{ij} for C, N, O and P atoms; x, y, z in riding mode for H atoms); 538 variables and 8283 observations with $I > 2.0\ \sigma(I)$; calcd $w = 1/[\sigma^2(F_o^2) + (0.0942P)^2 + 8.1397P]$ where $P = (F_o^2 + 2F_c^2)/3$, with the resulting R = 0.0823, R_W = 0.2412 and S_W = 1.036, $\Delta\rho < 0.677$ e Å^{-3}.

Single crystals of **4a** suitable for X-ray analysis were obtained by slow diffusion of *n*-hexane into a dichloromethane solution of the complex. Crystal data: $C_{30}H_{35}Cl_2F_3N_3O_4PRu$, M_r = 761.56 g mol^{-1}, monoclinic, space group $P2_1/n$, a = 15.3065(6) Å, b = 13.8547(5) Å, c = 15.6247(6) Å, β = 94.198(2)°, V = 3304.6(2) Å^3, Z = 4, D_x = 1.531 g cm^{-3}, μ = 0.740 mm^{-1}, F(000) = 1552, T = 120(2) K. The sample (0.080 × 0.100 × 0.100 mm) was studied on a Bruker APEX-II CCD using Mo-K$_\alpha$ radiation (λ = 0.71073 Å). The data collection ($2\theta_{max}$ = 27.921°, omega scan frames by using 0.7° omega rotation and 30 s per frame, range *hkl*: *h* −20,20 *k* −18,18 *l* −20,20) gave 98 790 reflections. The structure was solved with SHELXT-2014/5,[20] which revealed the non-hydrogen atoms of the molecule. After anisotropic refinement, all of the hydrogen atoms

Published on 25 May 2021. Downloaded by Goteborgs Universitet on 9/1/2021 8:25:04 AM.

were found with a Fourier difference map. The structure was refined with SHELXL-2018/3[21] using the full-matrix least-square techniques (the use of F square magnitude; x, y, z, β_{ij} for C, Cl, F, N, O, P and Ru atoms; x, y, z in riding mode for H atoms); 402 variables and 7227 observations with $I > 2.0\sigma(I)$; calcd $w = 1/[\sigma^2(F_o^2) + (0.0278P)^2 + 3.8006P]$ where $P = (F_o^2 + 2F_c^2)/3$, with the resulting $R = 0.0282$, $R_W = 0.0692$ and $S_W = 1.048$, $\Delta\rho < 0.926$ e Å^{-3}.

Single crystals of **4b** suitable for X-ray analysis were obtained by slow diffusion of *n*-hexane into a dichloromethane solution of the complex. Crystal data: $C_{30}H_{38}Cl_2N_3O_5PRu$, $M_r = 723.57$ g mol^{-1}, monoclinic, space group $P2_1/n$, $a = 11.2342(6)$ Å, $b = 17.0441(10)$ Å, $c = 16.4074(8)$ Å, $\beta = 92.713(2)^\circ$, $V = 3138.1(3)$ Å^3, $Z = 4$, $D_x = 1.532$ g cm^{-3}, $\mu = 0.764$ mm^{-1}, $F(000) = 1488$, $T = 120(2)$ K. The sample ($0.180 \times 0.150 \times 0.120$ mm) was studied on a Bruker PHOTON-III CPAD using Mo-K$_\alpha$ radiation ($\lambda = 0.71073$ Å). The data collection ($2\theta_{max} = 27.932^\circ$, omega scan frames by using 0.7° omega rotation and 30 s per frame, range *hkl*: h −14,14 k −22,22 l −21,21) gave 99 843 reflections. The structure was solved with SHELXT-2014/5,[20] which revealed the non-hydrogen atoms of the molecule. After anisotropic refinement, all of the hydrogen atoms were found with a Fourier difference map. The structure was refined with SHELXL-2018/3[21] by the full-matrix least-square techniques (the use of F square magnitude; x, y, z, β_{ij} for C, Cl, N, O, P and Ru atoms; x, y, z in riding mode for H atoms); 392 variables and 6696 observations with $I > 2.0\sigma(I)$; calcd $w = 1/[\sigma^2(F_o^2) + (0.0252P)^2 + 8.1733P]$ where $P = (F_o^2 + 2F_c^2)/3$, with the resulting $R = 0.0417$, $R_W = 0.0948$ and $S_W = 1.081$, $\Delta\rho < 1.565$ e Å^{-3}.

CCDC 2076187 (**3b**), 2076185 (**4a**) and 2076186 (**4b**).‡

Computational details

All calculations were performed using the Gaussian 09 program,[22] using the functional ωB97XD. Dispersion corrections were included.[23] All atoms were described using the 6-31+G** basis set except the ruthenium atom described by the SDD basis set and the associated pseudopotential. The structure was fully optimised and the wavefunction saved. The free enthalpy was extracted from the frequency calculations performed on this geometry. The weak interactions were studied through the NCI analysis[24] of the Gaussian wavefunction. All calculations were performed in the gas phase.

Conflicts of interest

There are no conflicts to declare.

Acknowledgements

We gratefully acknowledge the University of Carthage and the Tunisian Ministry of Higher Education and Scientific Research for the financial support (grant for S. H.).

Notes and references

1 (*a*) J. H. Meyer and P. A. Bartlett, *J. Am. Chem. Soc.*, 1998, **120**, 4600–4609; (*b*) M. Emgenbroich and G. Wulff, *Chem. – Eur. J.*, 2003, **9**, 4106–4117; (*c*) A. K. Bhattacharya, D. S. Raut, K. C. Rana, I. K. Polanki, M. S. Khan and S. Iram, *Eur. J. Med. Chem.*, 2013, **66**, 146–152; (*d*) A. K. Bhattacharya, D. S. Raut, K. C. Rana, I. K. Polanki, M. S. Khan and S. Iram, *Eur. J. Med. Chem.*, 2013, **66**, 146–152; (*e*) G.-Y. Yao, M.-Y. Ye, R.-Z. Huang, Y.-J. Li, Y.-M. Pan, Q. Xu, Z.-X. Liao and H.-S. Wang, *Bioorg. Med. Chem. Lett.*, 2014, **24**, 501–507; (*f*) S. A. R. Mulla, M. Y. Pathan, S. P. Gample and D. Sarkar, *RSC Adv.*, 2014, **4**, 7666–7672; (*g*) R. Damiche and S. Chafaa, *J. Mol. Struct.*, 2017, **1130**, 1009–1017; (*h*) Z.-G. Zeng, N. Liu, F. Lin, X.-Y. Jiang and H.-H. Xu, *Mol. Diversity*, 2019, **23**, 393–401; (*i*) Z. Radai, *Phosphorus, Sulfur Silicon Relat. Elem.*, 2019, **194**, 426–437.

2 (*a*) J.-L. Song and J.-G. Mao, *J. Solid State Chem.*, 2005, **178**, 3514–3521; (*b*) B. Zurowska and B. Boduszek, *Mater. Sci.*, 2011, **29**, 105–111; (*c*) B. Zurowska, K. Ślepokura, U. Kalinowska-Lis and B. Boduszek, *Inorg. Chim. Acta*, 2012, **384**, 143–148.

3 (*a*) M. Juribašić, K. Molčanov, B. Kojić-Prodić, L. Bellotto, M. Kralj, F. Zani and L. Tušek-Božić, *J. Inorg. Biochem.*, 2011, **105**, 867–879; (*b*) B. Zurowska, A. Brzuszkiewicz and B. Boduszek, *J. Mol. Struct.*, 2012, **1028**, 222–226.

4 B. Zurowska, A. Brzuszkiewicz and B. Boduszek, *Inorg. Chim. Acta*, 2013, **394**, 159–163.

5 (*a*) G. A. Pinna, G. Murineddu, C. Murruzzu, V. Zuco, F. Zunino, G. Cappelletti, R. Artali, G. Cignarella, L. Solano and S. Villa, *ChemMedChem*, 2009, **4**, 998–1009; (*b*) P. K. Parikh, H. M. Marvaniya and D. J. Sen, *Int. J. Drug Dev. Res.*, 2011, **3**, 248–255; (*c*) K. P. Harish, K. N. Mohana, L. Mallesha and B. N. Prasanna Kumar, *Eur. J. Med. Chem.*, 2013, **65**, 276–283; (*d*) V. R. Pidugu, N. S. Yarla, S. R. Pedada, A. M. Kalle and A. K. Satya, *Bioorg. Med. Chem.*, 2016, **24**, 5611–5617; (*e*) G. Karabanovich, J. Němeček, L. Valášková, A. Carazo, K. Konečná, J. Stolaříková, A. Hrabálek, O. Pavliš, P. Pávek, K. Vávrová, J. Roh and V. Klimešová, *Eur. J. Med. Chem.*, 2017, **126**, 369–383; (*f*) N. Parizadeh, E. Alipour, S. Soleymani, R. Zabihollahi, M. R. Aghasadeghi, Z. Hajimahdi and A. Zarghi, *Phosphorus, Sulfur Silicon Relat. Elem.*, 2018, **193**, 225–231; (*g*) B. Liu, R. Li, Y. Li, S. Li, J. Yu, B. Zhao, A. Liao, Y. Wang, Z. Wang, A. Lu, Y. Liu and Q. Wang, *J. Agric. Food Chem.*, 2019, **67**, 1795–1806; (*h*) N. Takahashi, K. Hayashi, Y. Nakagawa, Y. Furutani, M. Toguchi, Y. Shiozaki-Sato, M. Sudoh, S. Kojima and H. Kakeya, *Bioorg. Med. Chem. Lett.*, 2019, **27**, 470–478; (*i*) A. H. Ananth, N. Manikandan, R. K. Rajan, R. Elancheran, L. K. M. Ramanathan, A. Bhattacharjee and S. Kabilan, *Chem. Biodiversity*, 2020, **17**, e1900659; (*j*) T. Biftu, D. F. Feng, G.-B. Liang, H. Kuo, X. Qian, E. M. Naylor, V. J. Colandrea, M. R. Candelore, M. A. Cascieri, L. F. Colwell, J. M. J. Forrest, G. J. Hom, D. E. MacIntyre, R. A. Stearns, C. D. Strader, M. J. Wyvratt, M. H. Fisher and A. E. Weber, *Bioorg. Med. Chem. Lett.*, 2000, **10**, 1431–1434.

 This journal is © The Royal Society of Chemistry and the Centre National de la Recherche Scientifique 2021

Published on 25 May 2021. Downloaded by Goteborgs Universitet on 9/1/2021 8:25:04 AM.

6 (*a*) M. Du and X.-H. Bu, *Bull. Chem. Soc. Jpn.*, 2009, **82**, 539–554; (*b*) L. Haiduc, *J. Coord. Chem.*, 2019, **72**, 2127–2159.
7 (*a*) X. Gong, P. K. Ng and W. K. Chan, *Adv. Mater.*, 1998, **10**, 1337–1340; (*b*) W. K. Chan, P. K. Ng, X. Gong and S. Hou, *Appl. Phys. Lett.*, 1999, **75**, 3920–3922; (*c*) P. K. Ng, X. Gong, S. H. Chan, L. S. M. Lam and W. K. Chan, *Chem. – Eur. J.*, 2001, **7**, 4358–4367; (*d*) C.-Y. Wong, C.-M. Che, M. C. W. Chan, J. Han, K.-H. Leung, D. L. Phillips, K.-Y. Wong and N. Zhu, *J. Am. Chem. Soc.*, 2005, **127**, 13997–14007; (*e*) N. J. Lundin, P. J. Walsh, S. L. Howell, A. G. Blackman and K. C. Gordon, *Chem. – Eur. J.*, 2008, **14**, 11573–11583; (*f*) J. Wu, H.-Y. Li, L.-C. Kang, D.-P. Li, Q.-L. Xu, Y.-C. Zhu, Y.-M. Tao, Y.-X. Zheng, J.-L. Zuo and X.-Z. You, *J. Organomet. Chem.*, 2010, **695**, 2048–2056; (*g*) Y.-J. Liu and Y.-P. Zhang, *Z. Anorg. Allg. Chem.*, 2013, **639**, 533–537.
8 (*a*) V. J. Catalano and T. J. Craig, *Inorg. Chem.*, 2003, **42**, 321–334; (*b*) C.-H. Lin, H.-C. Kao, C.-J. Hsu and W.-J. Wang, *J. Chin. Chem. Soc.*, 2010, **57**, 1167–1171; (*c*) P. Florindo, I. J. Marques, C. D. Nunes and A. C. Fernandes, *J. Organomet. Chem.*, 2014, **760**, 240–247; (*d*) J. Pazinato, O. M. Cruz, K. P. Naidek, A. R. A. Pires, E. Westphal, H. Gallardo, E. Baubichon-Cortay, M. E. M. Rocha, G. R. Martinez, S. M. B. Winnischofer, A. Di Pietro and H. Winnischofer, *Eur. J. Med. Chem.*, 2018, **148**, 165–177.
9 (*a*) A. Mishra, S. C. Kang and K.-W. Chi, *Eur. J. Inorg. Chem.*, 2013, 5222–5232; (*b*) G. Süss-Fink, *J. Organomet. Chem.*, 2014, **751**, 2–19; (*c*) A. K. Singh, D. S. Pandey, Q. Xu and P. Braunstein, *Coord. Chem. Rev.*, 2014, **270–271**, 31–56; (*d*) P. Kumar, R. K. Gupta and D. S. Pandey, *Chem. Soc. Rev.*, 2014, **43**, 707–733; (*e*) P. Crochet and V. Cadierno, *Dalton Trans.*, 2014, **43**, 12447–12462; (*f*) L. Biancalana, G. Pampaloni and F. Marchetti, *Chimia*, 2017, **71**, 573–579; (*g*) L. Zeng, P. Gupta, Y. Chen, E. Wang, L. Ji, H. Chao and Z.-S. Chen, *Chem. Soc. Rev.*, 2017, **46**, 5771–5804.
10 (*a*) A. Fujii, S. Hashiguchi, N. Uematsu, T. Ikariya and R. Noyori, *J. Am. Chem. Soc.*, 1996, **118**, 2521–2522; (*b*) T. Ohkuma, M. Koizumi, H. Doucet, T. Pham, M. Kozawa, K. Murata, E. Katayama, T. Yokozawa, T. Ikariya and R. Noyori, *J. Am. Chem. Soc.*, 1998, **120**, 13529–13530; (*c*) K. Everaere, A. Mortreux and J.-F. Carpentier, *Adv. Synth. Catal.*, 2003, **345**, 67–77; (*d*) T. Ikariya and A. J. Blacker, *Acc. Chem. Res.*, 2007, **40**, 1300–1308; (*e*) B. Stefane and F. Pozgan, *Top Curr. Chem.*, 2016, **374**, 18; (*f*) D. A. Hey, R. M. Reich, W. Baratta and F. Kühn, *Coord. Chem. Rev.*, 2018, **374**, 114–132; (*g*) J. M. Gichumbi and H. B. Friedrich, *J. Organomet. Chem.*, 2018, **866**, 123–143; (*h*) A. Mannu, A. Grabulosa and S. Baldino, *Catalysts*, 2020, **10**, 162.
11 P. Niu, J. Kang, X. Tian, L. Song, H. Liu, J. Wu, W. Yu and J. Chang, *J. Org. Chem.*, 2015, **80**, 1018–1024.
12 (*a*) A. N. Pudovik, *Dokl. Akad. Nauk SSSR*, 1950, **73**, 499–502; (*b*) A. N. Pudovik, *Dokl. Akad. Nauk SSSR*, 1952, **83**, 865–868.
13 R. Wan, P. Wang, F. Han, Y. Wang and J. Zhang, *Synth. Commun.*, 2011, **41**, 864–870.
14 C. Fiore, I. Sovic, S. Lukin, I. Halasz, K. Martina, F. Delogu, P. C. Ricci, A. Porcheddu, O. Shemchuk, D. Braga, J.-L. Pirat, D. Virieux and E. Colacino, *ACS Sustainable Chem. Eng.*, 2020, **8**, 18889–18902.
15 I. Khan, A. Ibrar and J. Simpson, *CrystEngComm*, 2014, **16**, 164–174.
16 (*a*) B. Çetinkaya, S. Demir, I. Özdemir, L. Toupet, D. Sémeril, C. Bruneau and P. H. Dixneuf, *Chem. – Eur. J.*, 2003, **9**, 2323–2330; (*b*) S. Balaji, M. K. M. Subarkhan, R. Ramesh, H. Wang and D. Sémeril, *Organometallics*, 2020, **39**, 1366–1375; (*c*) S. Saranya, R. Ramesh and D. Sémeril, *Organometallics*, 2020, **39**, 3194–3201.
17 (*a*) P. Melle, J. Thiede, D. A. Hey and M. Albrecht, *Chem. – Eur. J.*, 2020, **26**, 13226–13234; (*b*) Z. Hao, K. Liu, Q. Feng, Q. Dong, D. Ma, Z. Han, G.-L. Lu and J. Lin, *Chin. J. Chem.*, 2021, **39**, 121–128; (*c*) D. Bhattacharyya, B. K. Sarmah, S. Nandi, H. K. Srivastava and A. Das, *Org. Lett.*, 2021, **23**, 869–875.
18 (*a*) D. J. M. Snelders, G. van Koten and R. J. M. Klein Gebbink, *J. Am. Chem. Soc.*, 2009, **131**, 11407–11416; (*b*) L. Monnereau, D. Sémeril, D. Matt and L. Toupet, *Chem. – Eur. J.*, 2010, **16**, 9237–9247.
19 L. Kathuria, N. U. Din Reshi and A. G. Samuelson, *Chem. – Eur. J.*, 2020, 7622–7630.
20 G. M. Sheldrick, *Acta Crystallogr., Sect. A: Found. Adv.*, 2015, **71**, 3–8.
21 G. M. Sheldrick, *Acta Crystallogr., Sect. C: Struct. Chem.*, 2015, **71**, 3–8.
22 M. J. Frisch, G. W. Trucks, H. B. Schlegel, G. E. Scuseria, M. A. Robb, J. R. Cheeseman, G. Scalmani, V. Barone, B. Mennucci, G. A. Petersson, H. Nakatsuji, M. Caricato, X. Li, H. P. Hratchian, A. F. Izmaylov, J. Bloino, G. Zheng, J. L. Sonnenberg, M. Hada, M. Ehara, K. Toyota, R. Fukuda, J. Hasegawa, M. Ishida, T. Nakajima, Y. Honda, O. Kitao, H. Nakai, T. Vreven, J. A. Montgomery Jr, J. E. Peralta, F. Ogliaro, M. Bearpark, J. J. Heyd, E. Brothers, K. N. Kudin, V. N. Staroverov, R. Kobayashi, J. Normand, K. Raghavachari, A. Rendell, J. C. Burant, S. S. Iyengar, J. Tomasi, M. Cossi, N. Rega, J. M. Millam, M. Klene, J. E. Knox, J. B. Cross, V. Bakken, C. Adamo, J. Jaramillo, R. Gomperts, R. E. Stratmann, O. Yazyev, A. J. Austin, R. Cammi, C. Pomelli, J. W. Ochterski, R. L. Martin, K. Morokuma, V. G. Zakrzewski, G. A. Voth, P. Salvador, J. J. Dannenberg, S. Dapprich, A. D. Daniels, O. Farkas, J. B. Foresman, J. V. Ortiz, J. Cioslowski and D. J. Fox, *Gaussian 09, Revision D.01*, Gaussian Inc., Wallingford CT, 2009.
23 S. Grimme, J. Antony, S. Ehrlich and H. Krieg, *J. Chem. Phys.*, 2010, **132**, 154104.
24 J. Contreras-Garcia, E. R. Johnson, S. Keinan, R. Chaudret, J.-P. Piquemal, D. N. Beratan and W. T. Yang, *J. Chem. Theory Comput.*, 2011, **7**, 625–632.